Temperature-Sensitive Aqueous Surfactant Two-Phase System Formation in Cationic−Anionic Surfactant Systems

Ke Wang,[†] Haiqing Yin,[†] Wei Sha,[†] Jianbin Huang,*[,†] and Honglan Fu[‡]

Beijing National Laboratory for Molecular Sciences (BNLMS), State Key Laboratory for Structural Chemistry of Unstable and Stable Species, College of Chemistry and Molecular Engineering, and College of Life Science, Peking University, Beijing 100871, P. R. China

Received: May 20, 2007; In Final Form: July 12, 2007

Temperature-induced aqueous surfactant two-phase system (T-ASTP), which was found to be of generic importance, was investigated in a series of conventional mixed cationic−anionic surfactant systems. On the basis of the investigations of turbidity, dynamic light scattering, transmission electron microscopy, and fluorescence resonance energy transfer, the formation of T-ASTP can be attributed to temperature-induced vesicle aggregation. Aggregated vesicles existed in the upper part, while the separated vesicles existed in the lower part. The phase separation temperature can be regulated by varying the surfactant composition or adding additives, such as D-sorbitol, urea, or NaBr. The hydrophobic interaction and cooperative effect between cationic and anionic surfactants played a significant role in the formation of T-ASTP.

Introduction

Aqueous mixtures of cationic and anionic surfactants exhibit interesting phase behaviors and properties, which mainly arise from electrostatic interactions between oppositely charged head groups. By adjusting composition, these interactions can be turned to produce various microstructures with characteristic geometries ranging from spherical to cylindrical to planar, which have been studied experimentally and theoretically in a lot of the literature.[1−4] However, usually more than one kind of aggregate existed in the solution, which endows the catanionic surfactant aqueous solutions with more complicated phase behaviors and makes the investigation more difficult and confusing.

The study of phase separation in colloid systems is a challenging work in statistical mechanics and has caused much interest in the past few decades.[5−16] The liquid−liquid phase-separation behavior, which was called "aqueous two-phase systems" (ATPS),[17−19] was first observed in polymer systems. Later, in some cationic−anionic mixed surfactant systems, a novel phenomenon in which two dilute liquid phases coexisted was also observed,[3,20−23] which opened a new area of surfactant applications in partitioning and analysis of biomaterials.[20] Previous research in catanionic surfactant solutions revealed that, at a certain mixed ratio and concentration, liquid−liquid phase separation can happen spontaneously, which was referred as the "aqueous surfactant two-phase systems" (ASTP).[20] In these systems, the phase separation with a clear interfacial boundary occurs spontaneously in a special region of the surfactants. Usually one phase of the ASTP is rich in surfactants and the other phase is poor. However, both of the two phases are the dilute aqueous solution of surfactants, and their volume ratio is dependent on the total surfactant concentration and the component. Although there have been many research reports dealing with ASTP phenomenon in surfactant solutions, the corresponding mechanism and driving force of ASTP formation are controversial due to the complexity and variety of phase behavior.

Normally, ASTP in catanionic surfactant solutions can be introduced by adjusting the mixed cationic/anionic surfactant ratio, total surfactant concentration, or adding electrolytes.[23] Temperature variation provides a quite simple way to tailor assemblies, and projects on temperature-sensitive systems have attracted the special attention of scientists.[24−32] Lower consolute behavior, i.e., phase separation on heating, is commonly observed in nonionic surfactant and water-soluble polymer solutions.[33−35] These micellar solutions become very turbid, and phase separation occurs at a threshold temperature, which is known as the cloud point. A similar phenomenon is rarely observed in ionic surfactant solutions, mainly because of the repulsive electrostatic effect between aggregates. On the basis of the previous literature, cloud point phenomenon was observed in several kinds of ionic surfactant system.[12−16,36−42] One contains large amounts of added electrolytes[42] that screen repulsive electrostatic effects. In a later study, another kind of ionic surfactant system with a large hydrophobic headgroup (e.g., surfactants or added salts with tributyl headgroup) was observed to display the cloud point phenomenon.[13−16] In addition, some ionic surfactants with an unsaturated long tail exhibit the cloud point phenomenon when a lower concentration of binding salt was added.[12,41] In this paper, temperature-sensitive ASTP (T-ASTP) was found in a series of conventional cationic−anionic mixed surfactant systems on heating. Different from previous research, T-ASTP was not only found for the surfactants with butyl headgroups, but also for those with smaller hydrophobic headgroups (e.g., propyl and even ethyl). Moreover, the solutions not only turned cloudy but also separated to form ASTP with a clear phase boundary on heating. The solution was a clear homogeneous solution with dispersed vesicles before the critical phase separation temperature, while it demixed to two phases when the temperature was above the critical value. The phase separation temperature (T_S) varied with the change

* Corresponding author. Fax: 86-10-62751708. Tel: 86-10-62753557. E-mail: JBHuang@pku.edu.cn.
[†] Beijing National Laboratory for Molecular Sciences.
[‡] College of Life Science.

10.1021/jp073903o CCC: $37.00
Published on Web 10/24/2007

Figure 1. Appearance of mixed solutions with the oil-soluble dye Sudan III (I) below the T_S and (II) above the T_S: (a) 50 mM 1:1.4 DBAB/SL, (b) 50 mM 1.3:1 DEAB/$SDSO_3$, and (c) 50 mM 1.3:1 DPAB/$SDSO_3$.

of catanionic mixtures, mixed ratio, or total surfactant concentration. The T-ASTP formation can be attributed to vesicle aggregation with the increase of temperature, and a stronger hydrophobic interaction of the polar head groups in cationic surfactants was proved to be beneficial to T-ASTP formation. External additives could adjust the hydrophobic interaction and control the phase separation temperature. A possible mechanism of T-ASTP formation is also discussed.

Experimental Section

Materials. Quaternary ammonium bromides including *n*-dodecyltributylammonium bromide (DBAB), *n*-dodecyltripropylammonium bromide (DPAB), and *n*-dodecyltriethylammonium bromide (DEAB) were prepared by reaction of 1-bromododecane and the corresponding trialkylamine. Sodium laurate (SL) was prepared by neutralizing lauric acid with NaOH in ethanol. Sodium *n*-dodecyl sulfate (SDS) and sodium *n*-dodecyl sulfonate ($SDSO_3$) were bought from Acros Organics Co. and Beijing Chemical Co., respectively. All the surfactants were recrystallized five times from mixed solvents of ethanol−acetone or ether−acetone. The purity of the surfactant was examined and no surface tension minimum was found in the surface tension curves. *N*-(7-Nitrobenz-2-oxa-1,3-diazol-4-yl)-1,2-dihexadecanoyl-*sn*-glycero-3-phosphoethanolamine, triethylammonium salt (NBD-PE), and Lissamine rhodamine B 1,2-dihexadecanoyl-*sn*-glycero-3-phosphoethanolamine triethylammonium salt (Rh-PE) were purchased form Invitrogen Molecular Probe Co. The water used was redistilled from potassium permanganate. The other reagents were the products of A. R. Grade. The cmc values of surfactants in aqueous solutions are shown in Table 1 of the Supporting Information.

Sample Preparation. Samples were prepared by mixing cationic and anionic surfactants at a desired concentration and mixing ratio. Samples were vortically mixed after sealing. If there is no special instruction, the pH of SL and cationic surfactant mixed system was fixed to 9.2 (0.01 M $Na_2B_4O_7 \cdot 10H_2O$) to control the hydrolysis of SL.

Turbidity Measurements. Turbidity measurements were carried out with a Shanghai 752C spectrophotometer at 514.5 nm. The temperature of turbidity measurement was controlled by an external thermostat.

DLS Measurements. Dynamic light scattering measurements were performed with a spectrometer (ALV-5000/E/WIN multiple tau digital correlator) and a Spectra-Physics 2017 200 mW Ar laser (514.5 nm wavelength). The scattering angle was 90°. The intensity autocorrelation functions were analyzed by using the Contin method, and the apparent hydrodynamic radius $\langle R_h \rangle$ was deduced from the diffusion coefficient D by the Stokes−Einstein formula $R_h = k_B T/(6\pi\eta D)$, where k_B is the Boltzmann constant and η is the solvent viscosity at T (K).

Transmission Electron Microscopy. Samples for TEM were prepared by the negative-staining technique with uranyl acetate water solution and by freeze−fracture replication according to standard techniques. Fracturing and replication were carried out in a high-vacuum freeze−etching system (Balzers BAF-400D). A JEM-100CX electron microscope was employed in the microscopic observation.

ζ-Potential Measurements. ζ-Potentials were measured using a temperature-controlled zetasizer 2000 (Malvern Instruments Ltd.).

Density Measurements. The densities of samples were measured by use of a density measurement system (Anton Paar DMA602 density measuring cell and DMA60 density meter).

Fluorescence Probe Experiment. The fluorescence resonance energy transfer (FRET) from NBD-PE to Rh-PE was measured using a Hitachi F4500 spectrofluorometer. The probe/surfactant molar ratio was 0.1%. The emission spectrum was recorded at a range of 475−700 nm with the excitation wavelength of 465 nm.

Results and Discussion

1. Phase Behavior. *1.1. Temperature-Sensitive ASTP Formation in the Solution of DBAB/SL.* At room temperature, the solution of 1:1.4 (mixed molar ratio) DBAB/SL with the total concentration of 50 mM was a clear, transparent, homogeneous solution. The solution will be a homogeneous phase with a clear or bluish appearance upon heating. However, when the temperature was increased to 39 °C, the solution turned cloudy and in a few minutes separated into a two-phase system with a clear phase boundary by eye observation. The upper phase showed no birefringent phenomenon through a polarization microscope and no viscoelastic property from rheological measurement. This T-ASTP solution also remixed to a homogeneous phase when the temperature was lower than 39 °C. This temperature of phase transition is named the phase separation temperature (T_S). The oil-soluble red dye Sudan III was added to make the separation process more visible, as Sudan III prefers to solubilize in the hydrophobic region of aggregates. Below the phase separation temperature (39 °C), the dye dispersed in the solution and the color of solution was pink (Figure 1.aI). After the formation of T-ASTP formed above 39 °C, the dye was concentrated in the upper phase and the color of the upper phase become dark red (Figure 1aII). When temperature fell below 39 °C, the solution appearance returned to the original state similar to that of Figure 1aI. Some relevant physical chemistry data were also measured to increase our understanding of ASTP. It can be found that the density of the upper phase (0.99303 g/mL) is lower than that of the lower phase (0.99616 g/mL), which is in coincidence with the solubilization result that the surfactants are rich in the

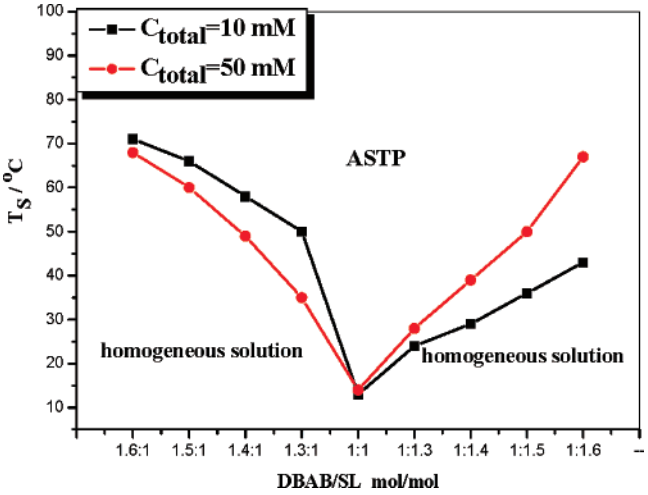

Figure 2. Phase separation temperatures (T_S) of DBAB/SL in different surfactant total concentration and mixed molar ratio. C_{total} = total concentration of surfactant.

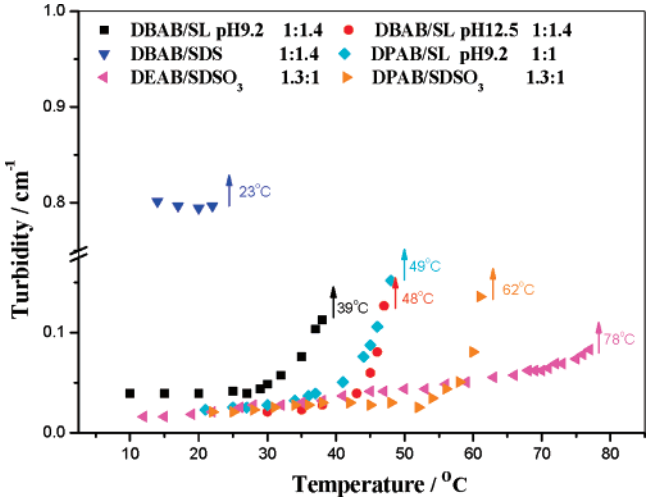

Figure 3. Turbidity heating curves for some mixed catanionic surfactant systems with the total concentration of 50 mM.

upper phase. Compared with the lower phase, the volume of the upper phase was only one-fifth of that of the lower one.

Other total surfactant concentrations and mixed ratios in the DBAB/SL system were also investigated, and temperature-induced ASTP was generally found in some region. Parts of the results are shown in Figure 2. It was interesting to find that some ASTP solutions formed at room temperature were also temperature-sensitive, because their T_S values were low enough. For instance, the T_S of 50 mM 1:1 DBAB/SL solution was only 14 °C. From Figure 2, it also can be found that the T_S in different solutions varies with the surfactant component and decreases with the mixed ratio approaching 1:1. Thus, it is convenient to adjust the T_S to the required temperature, which is very important to applications in biological extraction.

1.2. Temperature-Sensitive ASTP in Other Mixed Cationic−Anionic Surfactant Systems. Temperature-sensitive ASTP was also generally found in other different mixed catanionic surfactant systems, including a series of mixed systems with variation of cationic surfactant head groups or anionic surfactant head groups, such as DBAB/SL, DPAB/SL, DBAB/$SDSO_3$, DPAB/$SDSO_3$, DEAB/$SDSO_3$, DBAB/SL (pH = 12.5), and DBAB/SDS. It was a very novel phenomenon that temperature-induce ASTP formed in DEAB or DPAB systems. The appearance of some solutions in various systems with Sudan III is shown in Figure 1. After T-ASTP formation, the dye is rich in the upper phase in all solutions, demonstrating that the upper phase of solution is rich in surfactants.

Figure 3 presents the turbidity value upon heating in some mixed catanionic surfactant solutions. The arrows indicate the phase separation temperature of different aqueous systems. The tendency of turbidity variation upon heating is almost the same in all solutions. Below the phase separation temperature (T_S), turbidity values were almost constant as the temperature rose. Subsequently, as the temperature approached T_S, it increased slightly in some systems. However, when the temperature reached or exceeded T_S, the turbidity in all solutions began to increase obviously with time and ASTP was observed. After phase separation, turbidity of the upper phase was much higher than that of the lower phase. (For example, in the system of 50 mM 1:1.4 DBAB/SL, the turbidity value of the upper phase was 0.060 cm^{-1} and that of the lower one was 0.005 cm^{-1}.) This suggests that aggregates are bigger or more concentrated in the upper phase, which was essentially consistent with the dye solubilization results. On the other hand, the time needed for ASTP formation in various systems was greatly different. The different separation times are shown in Table 1. It can be noticed that the DBAB/SL system was more temperature-sensitive than any other systems. Possible reasons will be discussed in section 3.

TABLE 1: Values of ζ-Potential, Separation Time, and T_S for Different Cationic−Anionic Mixed Surfactant Systems with the Mixed Ratio of 1:1.4 at 50 mM

	ζ-potential, mV			
systems	20 °C	25 °C	separation time	T_S, °C
DBAB/SDS	−96.1	−	>1 month	23
DBAB/$SDSO_3$	−54.9	−51.8	about 10 days	37
DBAB/SL (pH 9.2)	−34.4	−34.2	within 2 h	39
DBAB/SL (pH 12.5)	−16.6	−16.3	within 2 h	48

2. Microstructures. *2.1. TEM and DLS.* Macroscopic phase behaviors are closely related to the microstructures in the aqueous solution. Therefore, microstructures of these catanionic mixtures were studied systemically. Unfortunately, the volume ratio of the upper phase to the lower one was very low in some solutions, which brought many difficulties to our investigation.

TEM and DLS techniques were also performed in several catanionic surfactant systems to investigate the microstructure variation in this process. In the system of 50 mM 1:1.4 DBAB/SL, TEM (Figure 4a) showed spherical vesicles in the homogeneous solution below T_S. Additionally, the DLS results of 50 mM 1:1.4 DBAB/SL at 25 °C (Figure 5a) revealed that there were two kinds of aggregates in this solution with an average hydrodynamic radius (R_h) of 6.9 and 50 nm, respectively, in this solution, which can be assigned to be micelle and vesicle, respectively, according to their sizes. The solution showed no viscoelastic property from rheological measurement and a low viscosity value similar to water. Therefore, it can be concluded that spherical vesicles and asymmetric short micelles coexisted in the solutions. During the process in which turbidity increased slightly with the temperature approaching 39 °C, both DLS and TEM results do not show obvious differences from those below 29 °C. After phase separation, the average R_h of the large aggregate in the upper part was 90 nm as determined by DLS, which was much larger than that of the lower part (25 nm) (Figure 5b). Vesicle aggregation and fusion in the upper part were confirmed by negative-staining TEM and FF-TEM (Figure 4b), indicating that the increase of turbidity was attributed to vesicle aggregation. On the contrary, only separated vesicles

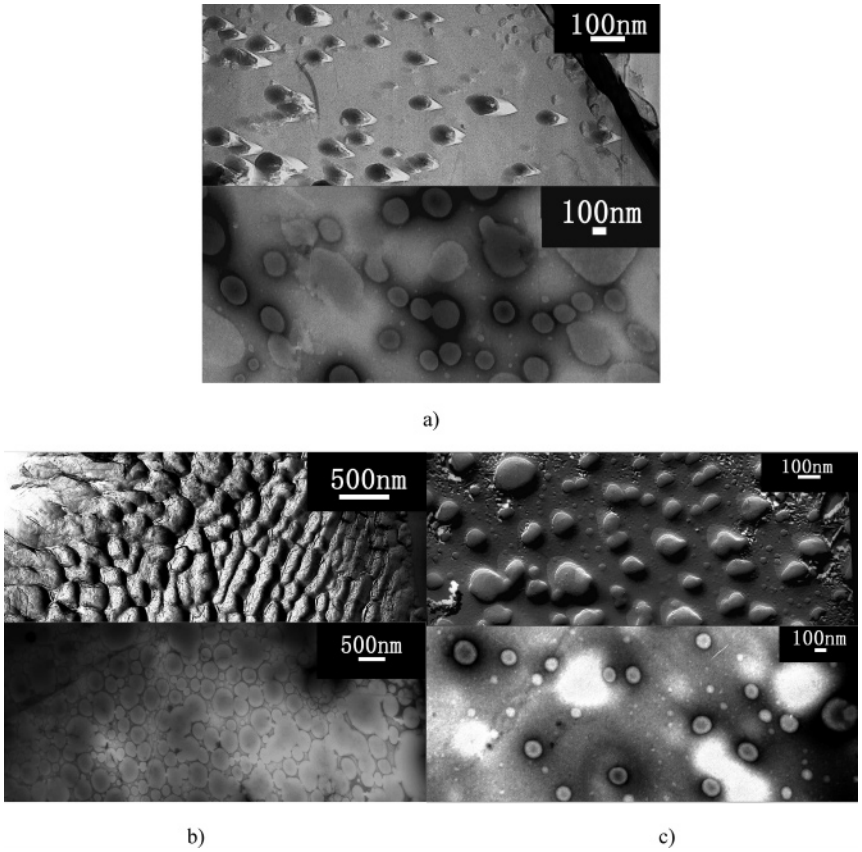

Figure 4. Micrographs for the 50 mM 1:1.4 DBAB/SL system before and after T-ASTP formation: (a) homogeneous solution at 25 °C (before T-ASTP formation), (b) the upper part of T-ASTP at 40 °C, and (c) the lower part of T-ASTP at 40 °C. Top: by FF-TEM technique; bottom, by negative-staining TEM technique.

were observed in the lower part (Figure 4c). TEM results of other solutions before and after T-ASTP formation are shown in Figure 6, which are similar to the case of 50 mM 1:1.4 DBAB/SL.

2.2 Fluorescence Assay. Vesicle aggregation and fusion can also be studied by fluorescence technique. The strong dependence of fluorescence resonance energy transfer (FRET) rate on intermolecular distance enables it to be one of the most effective methods of monitoring vesicle aggregation.[43−47] *N*-(7-Nitro-2,1,3-benzoxadiazol-4-yl) (NBD, energy donor) and rhodamine (Rh, energy acceptor) labeled phospholipids, are most commonly used for this purpose.[44−47] From the existing literature, there is a significant overlap between the emission band of NBD-PE and the excitation band of Rh-PE. If the two probes exist in close physical proximity, the energy from a photon absorbed by NBD-PE, the energy donor, can be transferred to Rh-PE, the energy acceptor, which will show directly excited fluorescence. Intensities for both NBD-PE and Rh-PE emissions (530 and 595 nm, respectively) were measured and reported as the ratio I_{595}/I_{530} to estimate the FRET efficiency.

After vesicles incorporated with NBD-PE and Rh-PE respectively were mixed in a 1:1 ratio, the fluorescence energy of NBD-PE transfer was observed, which may be due to the fast molecular exchange between vesicles in catanionic surfactant systems (inset in Figure 7). Unfortunately, this method cannot distinguish between vesicle aggregation and fusion correctly in our systems. Figure 7 shows the I_{595}/I_{530} value for the 50 mM 1:1.4 DBAB/SL system. The I_{595}/I_{530} value is almost invariable or decreases slightly when the solution was heated below T_S. After phase separation, the I_{595}/I_{530} value of the upper part increases remarkably (from 0.4 to about 0.6), while this value in the lower part decreases. Enhancement of the FRET efficiency

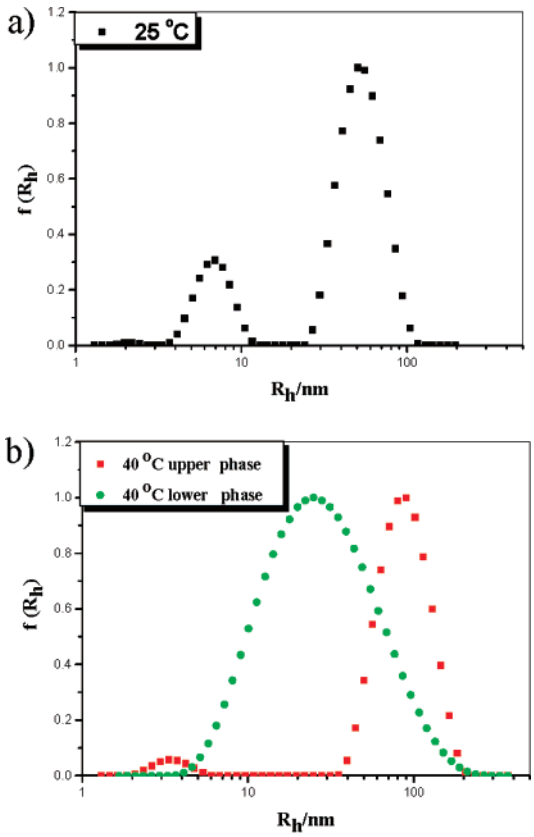

Figure 5. Hydrodynamic radius (R_h) distributions of 50 mM 1:1.4 DBAB/SL system: (a) before phase separation at 25 °C and (b) after phase separation at 40 °C.

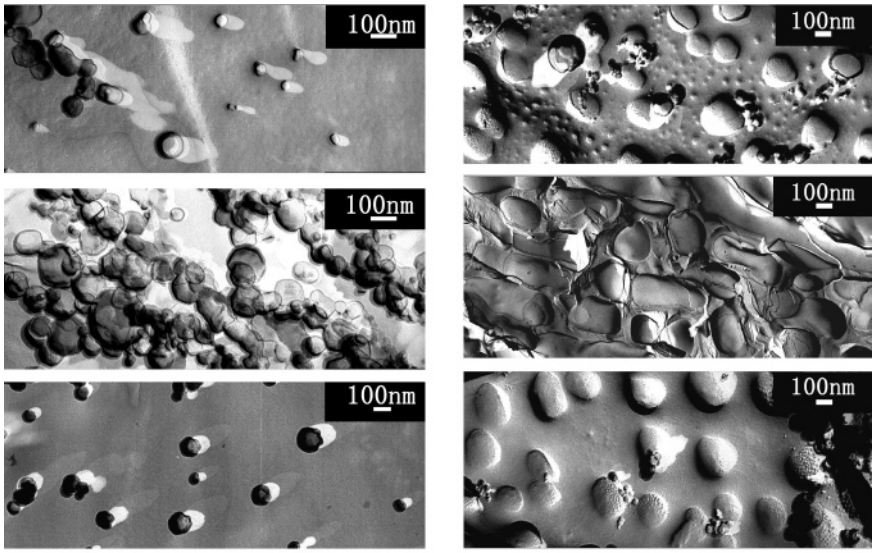

Figure 6. Micrographs by FF-TEM technique for different systems before and after T-ASTP formation: (a) 50 mM 1.3:1 DBAB/SL (T_S is 35 °C) and (b) 50 mM 1:1 DBAB/SL (T_S is 14 °C). Top, homogeneous solution; middle, upper part; bottom, lower part.

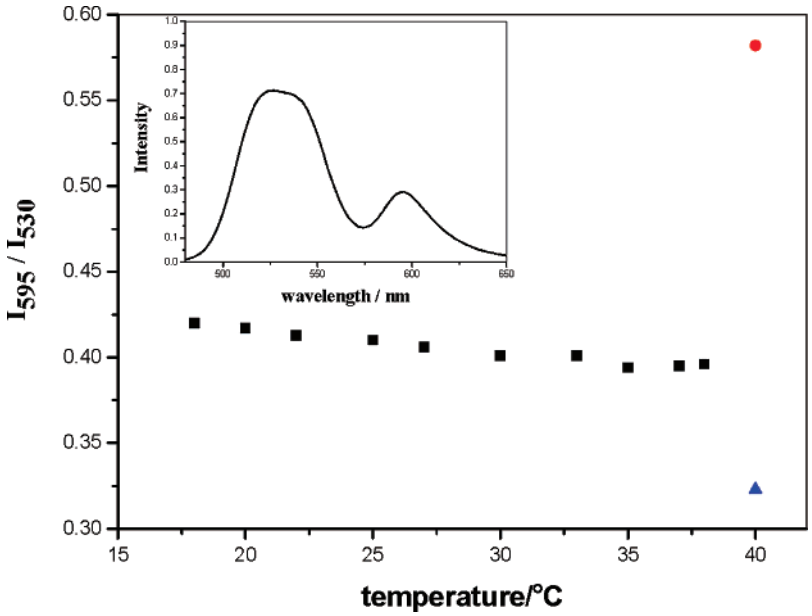

Figure 7. I_{595}/I_{530} value with temperature for the 50 mM 1:1.4 DBAB/SL system: homogeneous solution before phase separation (black square), the upper part (red circle), and the lower part (blue triangle) Fluorescence spectra at 25 °C is inset in the figure.

demonstrates that the two fluorophores are becoming closer and closer in spatial distance, which indicates that vesicles get together and aggregate. The larger I_{595}/I_{530} value revealed more aggregated vesicles, and aggregates became bigger in size. The fluorescence assay further supports the fact that vesicles aggregate in the upper part, which is also previously justified by TEM and other results.

Combining with the above results, it can be concluded that the T-ASTP formation is caused by temperature-induced vesicle aggregation. Usually, ASTP solution is not easily formed in ionic surfactant systems on heating because of the decrease or vanishing of aggregates. In ionic surfactant systems, the aggregate size normally decreases when the temperature increases, such as the transitions from vesicle to micelle.[27−29] The reverse process, which is the increase of aggregate size on heating, was rarely observed. However, temperature-induced vesicle aggregation, with the phenomenon of clouding on heating, was proved in the SDS/DBAB system before.[40] Therefore, it can be speculated that the process of vesicle aggregation is a key step for T-ASTP formation. However, T-ASTP could not form in all systems where vesicle aggregation occurred on heating. Possible reasons will be discussed in the following section.

3. Mechanism of Temperature-Sensitive ASTP Formation. Further research was performed to obtain more information about the mechanism of T-ASTP formation. It was found that the hydrophobic chain length in the polar head groups of cationic surfactants may play an important role in the process of T-ASTP formation. The mixed systems of SL with different cationic surfactants will be discussed in detail.

Similar to that observed in the system DBAB/SL, temperature-induced ASTP formation also occurred in DPAB/SL systems only with the comparatively higher T_S at the same composition, showing a narrower T-ASTP region in this mixed system (see the black section in Scheme 1). Investigation on microstructure variation also demonstrated that vesicle aggrega-

SCHEME 1: Mixed Molar Ratio Range of Temperature-Induced ASTP Formation in the Three Mixed Surfactant Systems of 50 mM[a]

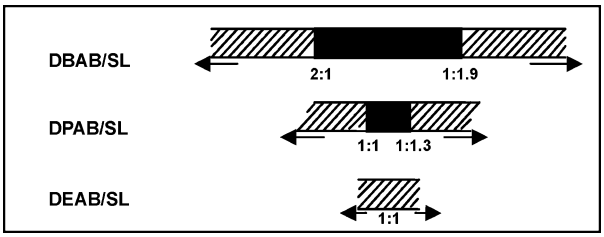

[a] Solid black: the area where temperature-induced ASTP formed without additives. Hatched pattern: the area where temperature-induced ASTP formed with additives that can enhance the hydrophobic interaction, like D-sorbitol.

tion occurred above T_S. For example, dispersed vesicles were observed in the homogeneous solution of 50 mM 1:1 DPAB/SL at 25 °C. As the temperature rose to above 49 °C (T_S for this mixed system), this solution demixed into two phases; aggregated vesicles in the upper part and dispersed vesicles in the lower part were observed respectively (Figure 8).

However, T-ASTP could not be observed in the DEAB/SL system, where the total surfactant concentration was less than 100 mM in any mixed ratio. It was noticed that the DPAB/SL system has much higher T_S than that of DBAB/SL in the same concentration and mixed ratio. Considering that the size sequence of the cationic surfactant polar head group is DBAB > DPAB > DEAB, it is possible to assume that the T_S for the DEAB/SL system is higher than that of the DPAB/SL system and beyond the range of measurable temperature.

Compared with the results in the systems DBAB/SL, DPAB/SL, and DEAB/SL, it can be found that T-ASTP will be easily formed in the mixed systems with bigger polar head groups or with longer hydrocarbon chains in the head group of cationic surfactants. The black section in Scheme 1 shows the mixed ratio range of T-ASTP formation in these three mixed systems, with the total surfactant concentration of 50 mM. The DBAB/SL system has the strongest ability to form ASTP on heating, followed by DPAB/SL, with the DEAB/SL system being weakest. This may be attributed to variation of the hydrophobic chains in the polar head group of cationic surfactant. The longer the hydrophobic chains are, the stronger the hydrophobic interaction becomes. Considering the steric restriction, at least one of the three hydrophobic chains in the cationic polar head groups must be exposed to the water outside the vesicle (Scheme 2). From the viewpoint of energy, it is unfavorable for the hydrocarbon chains to directly contact water, due to the hydrophobic effect. Therefore, the hydrophobic chains in different vesicles have the tendency to close up to each other, which induces vesicle aggregation and ASTP formation. Referring to our previous work and other literature,[15−16,37,40] hydrophobic interaction played a key role in vesicle or micelle aggregation. Because of its longest hydrophobic chains in the cationic polar group, the DBAB/SL system has the strongest hydrophobic interaction and the greatest vesicle aggregation.

However, the weaker hydrophobic interaction can be compensated by adding additives, which can then promote the hydrophobic interaction. D-Sorbitol and urea are known to exert strong influence on hydrophobic interaction in solution. Normally, urea is considered as a "water-structure breaker" and can weaken hydrophobic interactions,[48−50] while D-sorbitol is considered as a "water-structure maker", strengthening hydrophobic interactions,[51−52] so they were used as additives to adjust the hydrophobic interaction in the mixed surfactant solution in order to confirm the foregoing conclusion. If the additive can enhance the hydrophobic interaction, the aggregation process is facilitated and the ASTP formation temperature (T_S) will decrease. As expected, D-sorbitol can promote the ASTP formation, but urea is not beneficial to it. For example, 10 mM D-sorbitol can reduce the T_S of 50 mM 1:1.4 DBAB/SL from 39 to 28 °C, while 2 M urea can increase the T_S of the corresponding system to 48 °C. Similar variation of the microstructure was also observed when temperature increased to T_S. When 10 mM D-sorbitol was added into the mixed system of 50 mM 1:1.4 DBAB/SL, aggregated and dispersed vesicles were also observed by TEM in the upper and lower parts respectively at 30 °C, while the solution without additive at this temperature remained a single phase and only separated vesicles were found. The solution with 2 M urea was still homogeneous and only dispersed vesicles could be observed by TEM at 40 °C. Similar effects of these two additives on phase behavior and microstructure were also observed in the mixed system of DPAB/SL.

More interestingly, T-ASTP could also be observed by adding D-sorbitol to the DEAB/SL system, where no ASTP was found before D-sorbitol addition. For instance, 10 mM D-sorbitol can decrease the T_S to 29 °C in 50 mM 1:1 DEAB/SL and the corresponding microstructures are shown in Figure 9. Similarly, D-sorbitol can also enlarge the range of temperature-induced ASTP in the systems DBAB/SL and DPAB/SL (Scheme 1).

The factor discussed above affects the possibility of vesicles to aggregate, as well as their ability to aggregate. However, not all vesicle aggregation will necessarily induce T-ASTP formation, and the time of complete ASTP formation in various systems is in great difference as well. It was noticed that in the same concentration of 50 mM and mixed ratio of 1:1.4, the ASTP of DBAB/SL (pH = 9.2 and 12.5) systems can separate completely within 2 h, but in the mixed systems of DBAB/$SDSO_3$ and DBAB/SDS, it will take about 10 days and more than 1 month to form ASTP, respectively. The ζ-potential of different systems in the same concentration and mixed ratio was also measured (Table 1). The ζ-potential of 50 mM 1:1.4 DBAB/SDS system at 25 °C was not measured, because its T_S was 23 °C. From Table 1, the value of the ζ-potential was almost independent of temperature[40] but is closely related to the rate of temperature-sensitive ASTP formation. It is well-known that the ζ-potential of solution reflects the density of surface charge of aggregates and that a high surface charge will hold back further vesicle aggregation. Considering that vesicle aggregation is the main reason for temperature-sensitive ASTP formation, it is understandable that the system with a smaller absolute potential value will form ASTP faster. Simple inorganic salts, such as NaBr, will usually screen the electrostatic interaction between surfactants; thus, they can reduce the surface charge of aggregates and make further vesicle aggregation easier. For example, when 3.5 mM NaBr was added to the system 50 mM 1:1.4 DBAB/$SDSO_3$, the ζ-potential decreased from −51.8 to −19.0 mV, and as expected, the time for complete ASTP formation was greatly reduced from about 10 days to less than 2 h.

According to previous reports, there was no clouding point phenomenon in conventional ionic surfactants with smaller headgroups, like DPAB and DEAB, probably because the hydrophobic chains in the headgroups were not long enough, and the hydrophobic interaction was weak. However, in our work, T-ASTP formation was observed in both DPAB and DEAB catanionic mixed systems. In addition, in contrast to the DBAB/water binary mixture (temperature of all concentration is above 55 °C, and the lowest concentration is above 10 wt

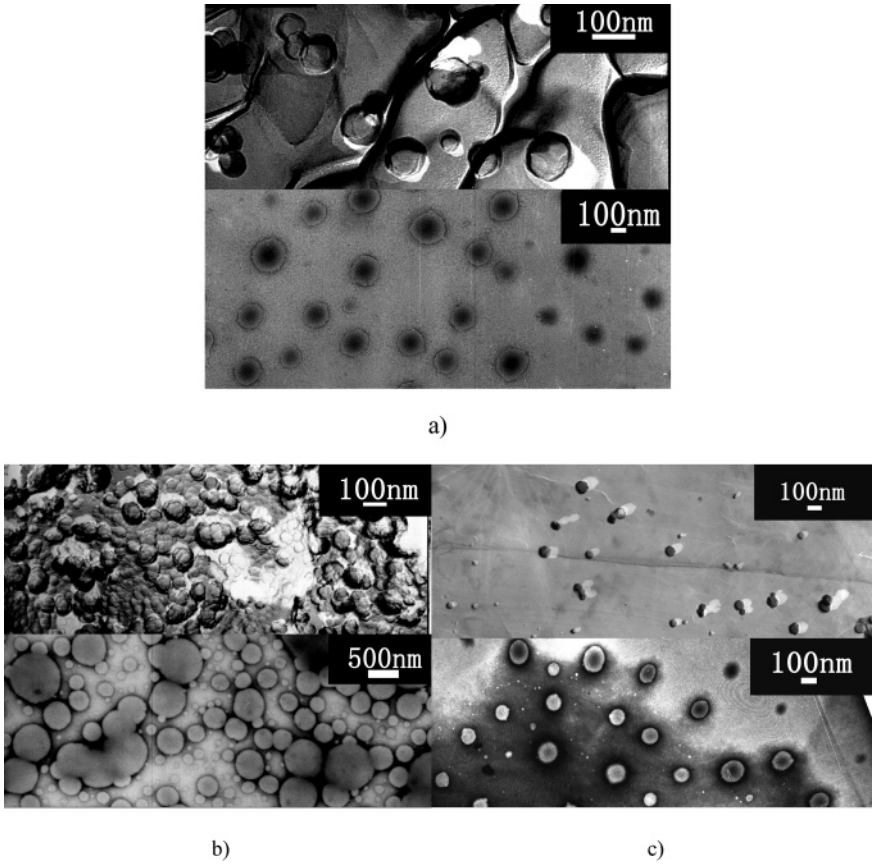

Figure 8. Micrographs for the system 50 mM 1:1 DPAB/SL before and after T-ASTP formation: (a) homogeneous solution at 25 °C (before T-ASTP formation), (b) the upper part of T-ASTP at 50 °C, and (c) the lower part of T-ASTP at 50 °C. Top, by FF-TEM technique; bottom, by negative-staining TEM technique.

SCHEME 2: Schematic Illustration of DBAB/SL Vesicle Membrane in Aqueous Solution

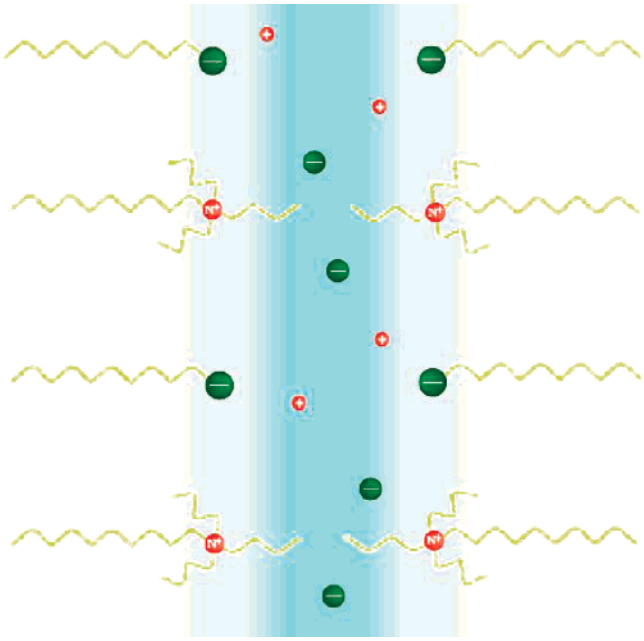

%),[14] solutions with butyl headgroups, DBAB/SL (pH = 9.2 and 12.5), DBAB/$SDSO_3$, and DBAB/SDS, present a much lower phase separation temperature. The interaction parameters β_m are shown in Table 1 in the Supporting Information. Obviously, the strong interaction between cationic and anionic surfactants was an important factor in T-ASTP formation.[53] The catanionic surfactants behave as a pair of "pseudo-nonionic" molecules. The closer the mixed ratio of surfactants approaches equimolar, the more obvious the nonionic character of aggregates will appear. In fact, the addition of inorganic salts can also decrease T_S, which screened the net surface charge of aggregates and made the vesicles nonionic. Such "pseudo-nonionic" phenomenon has been found in some catanionic micelle systems.[12,13,16,53,54]

On the basis of the differences in the structure of aggregates, the ASTP in catanionic surfactant systems can be usually divided into several classes. The entanglement of rodlike micelles,[20,21] the birefringent L_α phase,[3] or densely packed vesicles[22] could induce ASTP formation. Different aggregates in the two parts are the real reason for ASTP formation in nature. Combining the facts and analysis above, T-ASTP in our investigations could have a possible formation mechanism as follows. In the vesicle region of catanionic mixed surfactant systems, at a certain concentration and mixed ratio, vesicles can aggregate on heating when hydrophobic interactions and cat-anionic interactions come up to a certain degree. At the critical temperature, if the surface charge of vesicles is low enough, more and more vesicles aggregate with time. Then many aggregated vesicles form a type of three-dimensional network structure containing much water and the network structure separates from the original phase.[55] Compared with the other dispersed vesicles, the surface charge of aggregated vesicles was much closer to 1:1 and they combined much fewer counterions, which led to lower density. Therefore, the network structure composed of aggregated vesicles formed the upper part of ASTP. Scheme 3 demonstrates the process mentioned above, which is in accord with views on conventional ASTP formation.

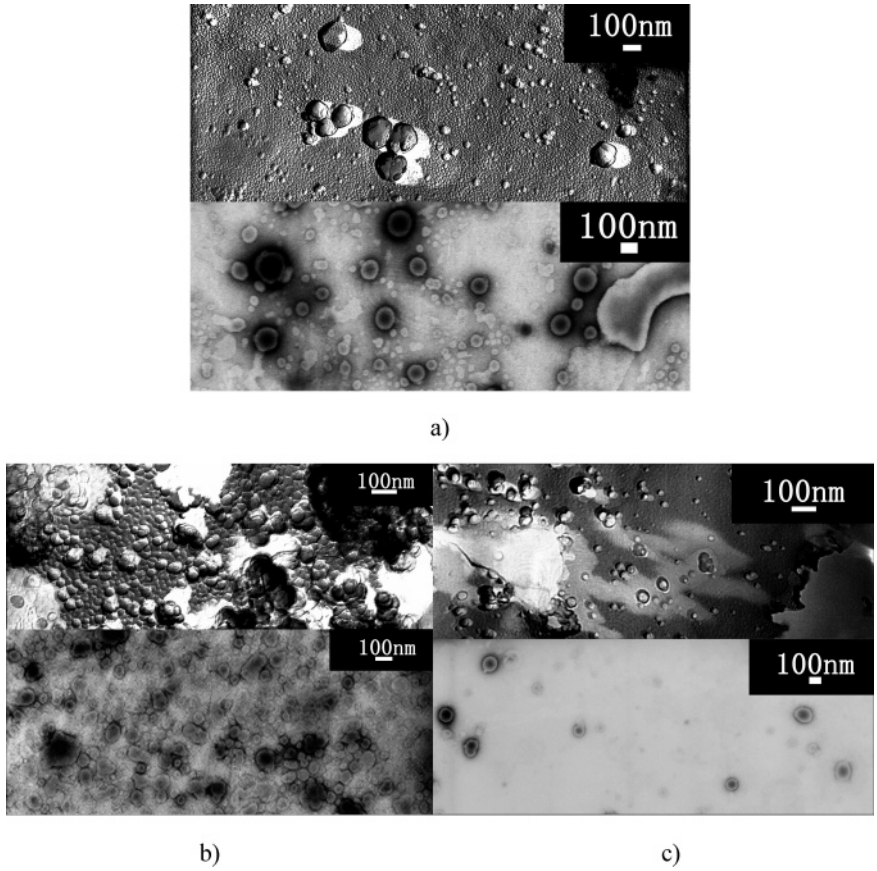

Figure 9. Micrographs for the 50 mM 1:1 DEAB/SL system with 10 mM D-sorbitol before and after T-ASTP formation: (a) homogeneous solution at 25 °C (before T-ASTP formation), (b) the upper part of T-ASTP at 30 °C, and (c) the lower part of T-ASTP at 30 °C. Top, by FF-TEM technique; bottom, by negative-staining TEM technique.

SCHEME 3: Representation of Temperature-sensitive ASTP Formation

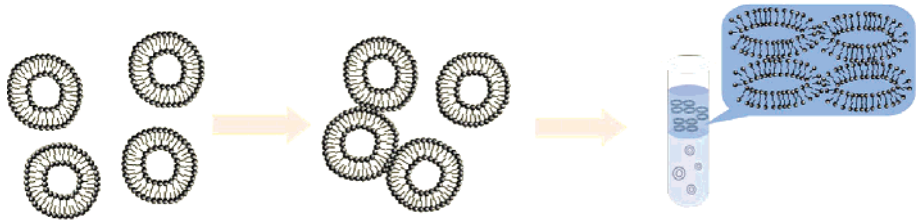

Conclusion

Temperature-sensitive ASTP, which can be attributed to temperature-induced vesicle aggregation, was generally found in a series of conventional cationic−anionic mixed surfactants systems. The process of T-ASTP formation can be divided into two steps. The first step was the transformation from vesicle to vesicle aggregation when the temperature reached the critical value T_S. By adjusting the surfactant species, total concentration, cationic/anionic mixed ratio, and the additives, the ability of vesicle aggregation can be changed and the T_S can be controlled. The second step was the process from vesicle aggregation to ASTP formation. The phase separation rate can be easily controlled by addition of inorganic salts (like NaBr). Our study on temperature-sensitive ASTP offers a simple and reversible way to control ASTP formation, which may advance its applications in biological extraction and other fields. Furthermore, the investigation of T-ASTP caused by vesicle aggregation might give us a greater understanding of the active control of self-assembly transformations and the relationship between macroscopic phase behavior and microscopic organized structures.

Acknowledgment. This work was supported by NSFC and the doctoral program of MOE in China.

Supporting Information Available: Cmc values and interaction parameters of surfactants in aqueous solutions. This material is available free of charge via the Internet at http://pubs.acs.org.

References and Notes

(1) Kaler, E. W.; Murthy, A. K.; Rodriguez, B. E.; Zasadzinski, J. A. *Science* **1989**,*245*,1371.
(2) Marques, E.; Khan, A.; da Graca Miguel, M.; Lindman, B. *J. Phys. Chem.* **1993**, *97*, 4729.
(3) Horbaschek, K.; Hoffmann, H.; Hao, J. C. *J. Phys. Chem. B* **2000**, *104*, 2781.
(4) Koehler, R. D.; Raghavan, S. R.; Kaler, E. W. *J. Phys. Chem. B* **2000**, *104*, 11035.
(5) Menger, F. M.; Peresypkin, A. V.; Caran, K. L.; Apkarian, R. P. *Langmuir* **2000**, *16*, 9113.
(6) Schmitz, K. S.; Bhuiyan, L. B. *Langmuir* **2002**, *18*, 1457.
(7) Linse, P.; Labaskin, V. *Phys. Rev. Lett.* **1999**, *83*, 4208.
(8) Imhof, A.; Dhont, J. K. G. *Phys. Rev. Lett.* **1995**, *75*, 1662.
(9) Steiner, U.; Meller, A.; Stavans, J. *Phys. Rev. Lett.* **1995**, *74*, 4750.
(10) Roux, D.; Knobler, C. M. *Phys. Rev. Lett.* **1988**, *60*, 373.

(11) Dinsmore, A. D.; Yodh, A. G.; Pine, D. J. *Nature* **1996**, *383*, 239.
(12) Raghavan, S. R.; Edlund, H.; Kaler, E. W. *Langmuir* **2002**, *18*, 1056.
(13) Yu, Z.-J.; Xu, G. *J. Phys. Chem.* **1989**, *93*, 7441.
(14) Warr, G. G.; Zemb, T. N.; Drifford, M. *J. Phys. Chem.* **1990**, *94*, 3086.
(15) Buckingham, S. A.; Garvey, C. J.; Warr, G. G. *J. Phys. Chem.***1993**, *97*, 10236.
(16) Kumar, S.; Sharma, D.; Kabir-Ud-Din. *Langmuir* **2000**, *16*, 6821.
(17) Posharnowa, N.; Schneider, A.; Wunsch, M.; Kuleznew, V.; Wolf, B. A. *J. Chem. Phys.* **2001**, *115*, 9536.
(18) Sear, R. P. *Phys. Rev. Lett.* **2001**, *86*, 4696.
(19) Tuinier, R.; Dhont, J. K. G.; De Kruif, C. G. *Langmuir* **2000**, *16*,-1497.
(20) Zhao, G.-X.; Xiao, J.-X. *J. Colloid Interface Sci.* **1996**, *177*, 513.
(21) Yatcilla, M. T.; Herrington, K. L.; Brasher, L. L.; Kaler, E. W. *J. Phys. Chem.* **1996**, *100*, 5874.
(22) Mao, M.; Huang, J. B.; Zhu, B. Y.; Ye, J. P. *J. Phys. Chem. B* **2002**, *106*, 219.
(23) Yin, H. Q.; Mao, M.; Huang, J. B.; Fu, H. L. *Langmuir*. **2002**, *18*, 9198.
(24) Bott, R.; Wolff, T.; Zierold, K. *Langmuir* **2002**, *18*, 2004.
(25) Gorski, N.; Kalus, J. *Langmuir* **2001**, *17*, 4211.
(26) Yin, H. Q.; Zhou, Z. K.; Huang, J. B.; Zheng, R.; Zhang, Y. Y. *Angew. Chem., Int. Ed.* **2003**, *42*, 2188.
(27) Mendes, E.; Oda, R.; Manohar, C.; Narayanan, J. *J. Phys. Chem. B* **1998**, *102*, *338.*
(28) Buwalda, R. T.; Stuart, M. C. A.; Engberts, J. B. F. N. *Langmuir* **2000**, *16*, 6780.
(29) Hassan, P. A.; Valaulikar, B. S.; Manohar, C.; Kern, F.; Bourdieu, L.; Candau, S. J. *Langmuir* **1996**, *12*,4350.
(30) Hoffmann, H.; Horbaschek, K.; Witte, F. *J. Colloid Interface Sci.* **2001**, *235*, 33.
(31) Majhi, P. R.; Blume, A. *J. Phys. Chem. B* **2002**, *106*, 10753.
(32) Inoue, T.; Motoyama, R.; Miyakawa, K.; Shimozawa, R. *J. Colloid Interface Sci.* **1993**, *156*, 311.
(33) Jonsson, B.; Lindman, B.; Holmberg, K.; Kronberg, B. *Surfactants and Polymers in Aqueous Solutions*; Wiley: New York, 1998.
(34) Brown, W.; Johnsen, R.; Stilbs, P.; Lindman, B. *J. Phys. Chem.* **1983**, *87*, 4548.
(35) Inoue, T.; Ohmura, H.; Murata, D. *J. Colloid Interface Sci.* **2003**, *258*, 374.
(36) Kumar, S.; Aswal, V. K.; Naqvi, A. Z.; Goyal, P. S.; Kabir-ud-Din *Langmuir* **2001**, *17*, 2549.
(37) Bales, B. L.; Zana, R. *Langmuir* **2004**, *20*, 1579.
(38) Zana, R.; Benrraou, M.; Bales, B. L. *J. Phys. Chem. B* **2004**, *108*, 18195.
(39) Yan, Y.; Li, L.; Hoffmann, H. *J. Phys. Chem. B* **2006**, *110*, 1949.
(40) Yin, H. Q.; Lin, Y. Y.; Huang, J. B.; Ye, J. P. *Langmuir* **2007**, *23*, 4225.
(41) Kalur, G. C.; Raghavan, S. R. *J. Phys. Chem. B* **2005**, *109*, 8599.
(42) Appell, J.; Porte, G. *J. Phys. (Paris) Lett.* **1983**, *44*, L689.
(43) Andrews, D. L.; Demidov, A. A. *Resonance Energy Transfer*; John Wiley & Sons Ltd: Chichester, 1999.
(44) Struck, D. K.; Hoekstra, D.; Pagano, R. E. *Biochemistry* **1981**, *20*, 4093.
(45) Rupert, L. A. M.; Hoekstra, D.; Engberts, J. B. F. N. *J. Am. Chem. Soc.* **1985**, *107*, 2628.
(46) Duzgunes, N.; Allen, T. M.; Fedor, J.; Papahadjopoulos, D. *Biochemistry* **1987**, *26*, 8435.
(47) Eum, K. M.; Riedy, G.; Langley, K. H.; Roberts, M. F. *Biochemistry* **1989**, *28*, 8206.
(48) Kresheck, G. C.; Scheraga, H. A. *J. Phys. Chem.* **1965**, *69*, 1704.
(49) Manabe, M.; Koda, M.; Shirahama, K. *J. Colloid Interface Sci.* **1980**, *77*, 189.
(50) Frank, H. S.; Franks, F. *J. Chem. Phys.* **1968**, *48*, 4746.
(51) Penfold, J.; Staples, E.; Tucker, I.; Cummins, P. *J. Colloid Interface Sci.* **1997**, *185*, 424.
(52) Staples, E.; Thompson, L.; Tucker, I.; Penfold, J.; Thomas, R. K.; Lu, J. R. *J. Colloid Interface Sci.* **1996**, *184*, 391.
(53) Nakama, Y.; Harusawa, F.; Murotani, I. *JAOCS* **1990**, *67*, 717.
(54) Mehreteab, A.; Loprest, F. J. *J. Colloid Interface Sci.* **1988**, *125*, 602.
(55) Drye, T. J.; Cates, M. E. *J. Chem. Phys*. **1992**, *96*, 1367.